ACS OMEGA

http://pubs.acs.org/journal/acsodf

Article

Wooden Polymer Composites of Poly(vinyl chloride), Olive Pits Flour, and Precipitated Bio-Calcium Carbonate

Salah F. Abdellah Ali,* Ibrahim O. Althobaiti, E. El-Rafey, and Ehab S. Gad

Cite This: *ACS Omega* 2021, 6, 23924–23933

Read Online

ACCESS | Metrics & More | Article Recommendations

ABSTRACT: As a filler to be inserted into poly(vinyl chloride) (PVC), low-cost olive pits flour (OPF) and precipitated bio-calcium carbonate (PBCC)-produced PVC/OPF/PBCC composites have been used with high stability and rigidity compared to PVC. Hydrogen bonding is generated between OH cellulose in OPF and H in PVC. Composite tensile modulus increased in PVC grid in the presence of PBCC and OPF, possibly because of a filler restriction effect on the polymer chains. The hardness also increased as both OPF and PBCC increased. The mechanical tendency of the PVC/OPF composite was improved by adding a low content of PBCC particles with the PVC network, resulting in a smart distribution in the range of 10% by weight, and it was reduced by adding more than that percentage. The successful distribution of PBCC in PVC/OPF composite strengthened the mechanical path. The morphology and possible interface adhesion of components in the composite were demonstrated by scanning electron microscopy (SEM). The PVC SEM images showed a homogeneous, smart, and consistent surface, while the PVC/60 wt % OPF SEM images showed a large number of voids that suggested weak PVC/OPF interactions. The SEM images showed outstanding PBCC distribution in the PVC/OPF matrix for the PVC/50 wt % OPF/10 wt % PBCC composite. Due to the accumulation of PBCC particles producing cavities, the distribution of particles became nonhomogeneous at percentages above 10 wt %. At a low filler material, better spread of PBCC particles in the PVC grid was achieved. Owing to the polarity of OPF, the H_2O absorption and thickness swelling of PVC/OPF/PBCC composites showed higher amounts than PVC. PBCC improved the thermal stabilization and the neutralization of Cl^- negative ions as an acid acceptor of secondary PVC stabilization.

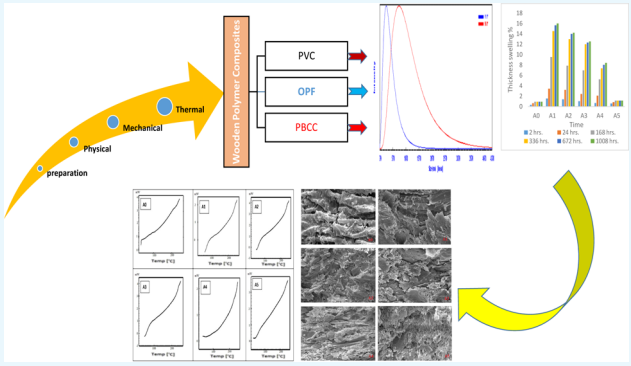

1. INTRODUCTION

Polymers are used in day-to-day life, namely, rubber, plastic, and resins and are labeled in accordance to their origin, such as natural rubber and silk, starch, semisynthetic modified polymers, cellulosic compounds, and synthetic ones (polyolefins, polystyrene, polyesters, polyethers, and PVC).[1−4] PVC is used in pipes, electric powered wires, window profiles, etc. It has proper mechanical properties, fire and fungus opposing and lengthy lifetime.[5−8] PVC produced by cracking from petroleum or natural gas bears a randomly disbursed molecular weight with a degree of viscosity with some additives that govern its physical, thermal, and mechanical characters and improve cost, processability, durability, weather resistance, color, and electrical performance.[9−11] Heat stabilizers like tribasic $PbSO_4$ and lead compounds increase thermal degradation concerning PVC, discoloration, and decay of both mechanical and chemical properties. Processing aids like methyl methacrylate (MMA) encourage the melt flow during manufacturing and improve the transparent look. Impact modifiers like chlorinated polyethylene (CPE) or acrylonitrile-butadiene-styrene terpolymer (ABS) rubbery copolymers are matching with PVC to increase impact strength and achieve ductility weathering.[12,13] Some additives act as lubricants to reduce the frictional resistance inside polymer matrix.[14] Antioxidants and stabilizers are free radicals' scavengers or phenol derivatives that can stop peroxide radicals from degrading hydroperoxide, change inactive derivatives via chemical reaction, and enhance both thermal and optical properties of PVC. Hydroxy-benzophenone and hydroxylphenyl triazole are considered as light stabilizers dissipating UV diffraction prior to degradation that prevent permanent chemical change.[15] Fillers exchange a partof plastic yet decrease cost, improve properties yet performance such as $CaCO_3$ filler in calcite mineral could be able to keep as grounded to a particular particle size.[11] Coated $CaCO_3$ with stearic acid, as a common cover of $CaCO_3$ that minimize longevity attention of wetness during storage and bulk agglomeration during the mixing

Received: June 4, 2021
Published: September 13, 2021

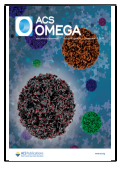

process, reduces interfacial tension, H_2O absorption, adsorption on processing aids, and impingement of polymer melt and then enhance melt flowing features.[16] Coated $CaCO_3$ with a common particle dimension of 1 μm has a positive effect on the impact strength of PVC to be used for window line production and many applications.[17] Fillers components have unique properties different from PVC relying on every component properties and the interface factors between components over last made-up production.[18] Natural fibers were used in high percentages in commercial WPC products to enhance durability, mechanical strength performance, interfacial quality of WPCs, the manufacturing rate, and reduces the rate of H_2O absorption.[19−23] Studies on PVC performance with some fibers and coupling agents are available.[24−29] As reinforcing materials, olive waste has rising potential among many other applications.[30−32] Cornwell showed that calcium carbonate increases the impact strength of PVC and proved it especially for PBCC in PVC.[33] This work aims at evaluating the effect of waste fiber (OPF) and PBCC on the physical, mechanical, thermal, and morphological properties of PVC to produce new costless WPCs and manage wastes that pollute the environment. Characterization of PVC/OPF/PBCC composites using SEM, FTIR, TGA, and DSC, as well as mechanical characters, water uptake, thickness swelling, and specific gravity measurements were done.

2. EXPERIMENTAL SECTION

2.1. Materials. PVC powder (K-value = 67, d: 5×10^{-2} to 56×10^{-2} g/mL, inherent viscosity = 92×10^{-2}) was provided by Egyptian Petrochemical Co. Chlorinated polyethylene (CPE) was introduced in PVC/OPF/PBCC composites as a toughening modifier to compatibilize polymer lattice with the filler enhancing melt process. Tribasic lead sulfate (TBLS), dibasic lead stearate (DLST), and lead stearate (NLST) have been utilized as thermal stabilizers; stearic acid, polyethylene wax, and calcium stearate (CaST) have been utilized as lubricants; titanium dioxide (TiO_2) has been used as a photoactive agent; and acrylic processing resource (K-120) has been used to facilitate processing.[34] All compounds were brought from Egyptian Petrochemical Co., Egypt. PBCC was extracted from the waste of beet juice extraction in the sugar industry using heat, H_2O, and CO_2 for purification, then dried at 105 ± 3 °C for 48 h, and finally shifted to a 100-mesh screen. OPF was prepared by grinding large amounts of olive pits in local workshops.

2.2. Preparation and Characterization. A compression molding device (Hexa Plast, India) was used to prepare PVC/OPF/PBCC composites at 170 °C and 140 bar producing 15 cm × 15 cm × 0.3 cm sheets to be tested for tensile (ASTM D638-03), flexural (ASTM D790-03), and Izod impact (ASTM D256-06a). PVC/OPF/PBCC composites were characterized by FTIR spectroscopy with KBr disk within 350−4400 cm^{-1} using PerkinElmer Spectrum BX model. The SEM model JEOL JSM-6360LA was utilized to signify the surface morphology on all PVC/OPF/PBCC compositions. The tensile test of dumbbell-shaped samples was matched with ASTM D638-03 using machine model—Zwick 2005. Notched-Izod impact of hollow die cutting having a thickness of about 3 mm according to ASTM D 256-06 was tested via a Ceast Izod impact model tester. The flexural strength test was done on bars having 80 × 10 × 3 mm with a three-point loading system (ASTM standard D 790-03). Three replicates on each composition have been tested. Shore-D-hardness was examined in accordance with ASTM standard D 2240-00 at a weight of 5 kg. Water uptake was measured according to ASTM standard D-570-98 by putting samples in distilled water at 23 ± 2 °C for different intervals from 2 h to 42 days and then weighed after drying. Three measurements have been made to calculate the amount of water uptake (%) as $[(W_2 - W_1)/W_1]$ x 100, where W_1 is the weight before immersing in H_2O and W_2 is the weight after immersing in H_2O.

Thickness swelling check was performed in accordance with British standard 373 using distilled H_2O at 23 ± 2 °C for different intervals between 2 h and 42 days and then dried and weighed. Specific gravity concerning whole composites was measured by a pycnometer in accordance with ASTM standard D 792.[35] Specific gravity (Sp.gr.) was calculated as $\text{Sp . gr.} = \frac{a}{(a+b-m)}$, where a is the sample weight, b is the weight of pycnometer filled with H_2O, and m is the weight of pycnometer with sample.

Thermogravimetric analysis (TGA) in accordance with ASTM D 3850-94-ASTM 2012 using a PerkinElmer device (TGA-50H) was performed between 25 and 500 °C with N_2 (g) surroundings at a rate of 10 °C/min in a Pt cell at the City of Scientific Research, Egypt. Differential scanning calorimetry (DSC) was performed in accordance with ASTM D 3418-03-ASTM 2012 in DSC, 60-A SHIMADZU. Each composite (5−10 mg) was positioned in Al capsules and then heated in the range of 25−250 °C under N_2 (g) flow at a rate of 5 °C min^{-1} at Polymer Lab., City of Scientific Research, Alexandria.[13]

3. RESULTS AND DISCUSSION

3.1. PBCC Analysis. $CaCO_3$ material content in PBCC was measured using volumetric techniques.[36] It gives 81.6 at 9.38% moisture content (ASTM D3030), a density of 0.745 g/mL (ASTM D1895), and a dioctyl phthalate, (DOP) uptake of 54/100 g (ASTM D3367). Evaluation was made at Polymer Lab at the Egyptian Petrochemical Co., Alexandria. Specimens were examined using a JEOL-JSM SEM for particles of two shapes of rod and sphere with dimensions of $(875-196) \times 10^{-3}$ and $(840-270) \times 10^{-3}$ μm (rod-shaped particles) and $(30-82) \times 10^{-3}$ μm (spherical-shaped particles) as shown in Figure 1. Different shapes may be generated under the effect of CO_2 injection rate and temperature during PBCC extraction.[13]

Laser diffraction measurement of PBCC particles distribution was done using a Beckman Coulter instrument with an M5-Submicron analyzer at City of Scientific Researches, Alexandria. Two particle size averages were obtained at two angles matching for the two shapes of PBCC particles, 351 nm at 11.1° and 898.5 nm at 90°, as explained in Figure 2. An EDX detector (JEOL JSM-6360LA) together with advanced vacuum technique was used to detect different elements and oxides in PBCC. Results are recorded in Figure 3 and explained in Tables 1 and 2.[13]

Two roll mill compression molding was utilized to prepare the proposed compositions. PVC compound without OPF and PBCC were mixed along with components in a TRL-20 C turbo mixer (5 L) at 2000 rpm and 115 °C, then cooled at 40 °C, cast to PE sacks, loaded with OPF and PBCC, and finally introduced to Betol Machinery Ltd., UK, at 180 °C to obtain PVC/OPF/PBCC sheets with different compositions as listed in Tables 3 and 4.[13,37]

3.2. OPF Analysis. OPF was analyzed in Table 5 using many different sieves to detect size distribution via opening size of 60 mesh with 42.37%, 80 mesh with 31.64%, 100 mesh with 12.43%, 140 mesh with 8.06%, 200 mesh with 3.72%, and remaining 1.78 wt %. The average particle size of OPF was 241.5

https://doi.org/10.1021/acsomega.1c02932
ACS Omega 2021, 6, 23924−23933

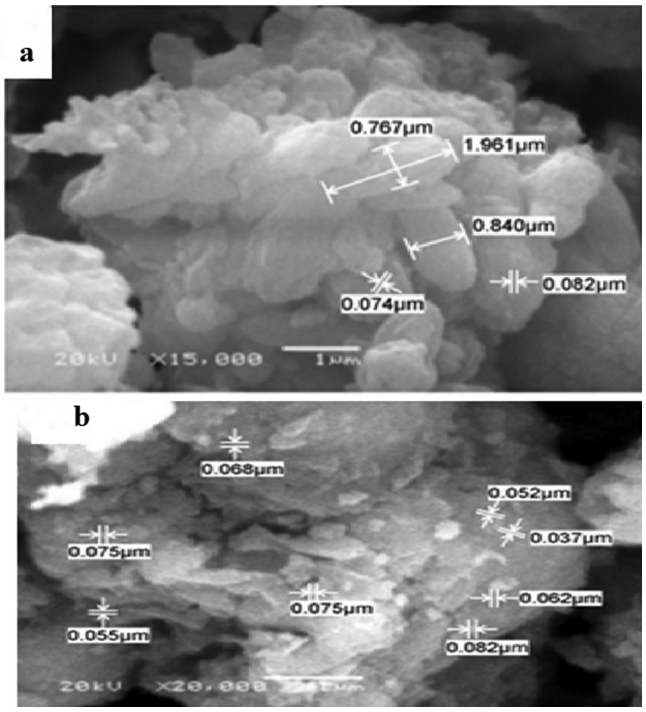

Figure 1. PBCC morphology with (a) 15 000× and (b) 20 000× magnification.

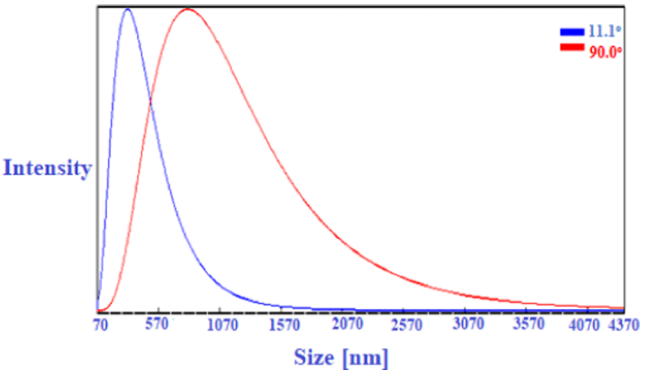

Figure 2. PBCC particle size distribution.

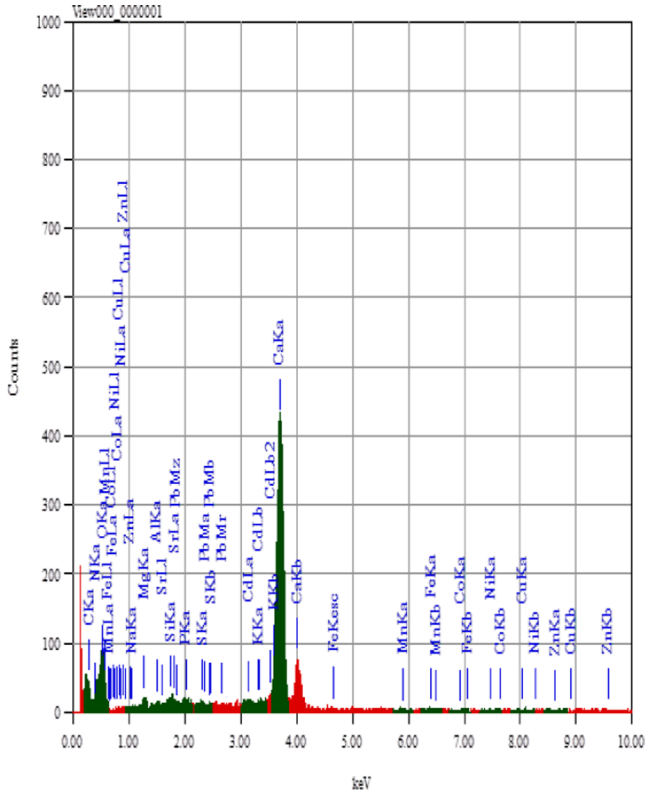

Figure 3. Analysis of PBCC elements.

Table 1. Elements Analysis of PBCC by EDX

element	wt %	element	wt %
carbon	11.15	chromium	0.06
oxygen	32.81	manganese	0.31
sodium	0.20	iron	0.43
magnesium	1.48	cobalt	0.32
aluminum	0.48	nickel	0.01
silicon	0.86	copper	0.45
phosphorus	0.74	zinc	0.38
sulfur	0.42	strontium	0.39
potassium	0.21	cadmium	0.08
calcium	49.13	lead	0.33

μm that dried at 105 ± 3 °C for 48 h to eliminate moisture as much as possible until reaching fixed weight in accordance with ASTM D-1037 at the Faculty of Agriculture, Alexandria University.

3.3. FTIR Spectra. Figure 4 shows the different functional groups of PVC, PBCC, and OPF, as well as the interactions of components in such compositions. PVC illustrates peaks at 616 cm^{-1} for C−Cl stretching vibration, 970 cm^{-1} for rocking CH_2, 1095 cm^{-1} for (C−C) stretching vibration, 1250 cm^{-1} for C−H stretching from CH−Cl, 1330 cm^{-1} for CH_2 deformation, 1430 cm^{-1} for wagging CH_2 group, 1734 cm^{-1} for carbonyl group, (in lubricants), and 2920 cm^{-1} for C−H asymmetric stretching vibration from CH−Cl. PBCC was featured at 3422 cm^{-1} that is assigned to moisture (−OH hydroxyl group stretching vibration), 2518 cm^{-1} in accordance with (C−H) aliphatic stretching vibration, 1796 cm^{-1} for (C═O) stretching vibration, 1429 cm^{-1} for (C−H) bending vibration, 1075 cm^{-1} for (C−O) stretching vibration because of the presence of sucrose, and 873 cm^{-1} for (C−O) bending vibration.

OPF gave a band around 3350 cm^{-1} for cellulosic (O−H) stretching, 2925 cm^{-1} for (C−H) symmetrical stretching vibration, 1745 cm^{-1} for (C═O) stretching, 1640 cm^{-1} for (C═C) stretching vibration, 1510 cm^{-1} for (C═C) aromatic skeletal vibrations, and 1405 cm^{-1} for (C−H) in cellulose and hemicellulose. The bands at 1110 and 1040 cm^{-1} were featured for (C−O) stretching. As appeared in A2, A5 spectra, the PVC peak at 1430 cm^{-1} was overlapped by the PBCC, indicative peak of intensity at 1426, 1427 cm^{-1} of (C−H) bending vibration owing to the wagging (CH_2) group. The presence of PBCC in PVC composites was demonstrated by a new peak assignment at 873 cm^{-1} that was caused by (C−O) bending vibration. Also, the peak of OPF around 3350 cm^{-1} for (O−H) stretching was shifted to a lower frequency (3410 cm^{-1}) upon adding to PVC. This is might be because of H bonds produced among −OH groups of cellulose/lignin in OPF and α-H in PVC, confirming an interaction between OPF and PVC.[13,38,39]

3.4. Morphological Characteristics. SEM results confirmed the morphology micrographs and interfacial interference of OPF and PBCC within PVC chains. Figures 5 and 6 show the

https://doi.org/10.1021/acsomega.1c02932
ACS Omega 2021, 6, 23924−23933

Table 2. Oxides Analysis in PBCC by EDX

oxides	wt %
sodium oxide	0.43
magnesium oxide	2.68
aluminum oxide	0.97
silicon oxide	2.01
phosphorus oxide	1.24
sulfur oxide	1.17
potassium oxide	0.29
chromium oxide	0.09
manganese oxide	0.45
ferrous oxide	0.61
cobalt oxide	0.3
nickel oxide	0.01
copper oxide	0.63
zinc oxide	0.33
strontium oxide	0.5
cadmium oxide	0.1
lead oxide	0.68

Table 3. PVC Components (PVC Compound)

type	Phr.
PVC	100
CPE	2
TBLS	3
DBLST	1
NLST	0.5
K120	1.5
Ca-stearate	0.5
stearic acid	1
polyethylene wax	1
TiO_2	1

Table 4. Compositions of Different PVC/OPF/PBCC Composites

samples	PVC	OPF	PBCC
A0	100		
A1	40	60	
A2	40	50	10
A3	40	40	20
A4	40	30	30
A5	40		60

Table 5. OPF Components Analysis

fiber	lignin (wt %)	cellulose (wt %)	hemicelluloses (wt %)	ash content (%)	average bulk, *d* (g/mL)
OPF	33.67	48.62	16.78	0.93	0.21

SEM micrographs of the fractured surfaces of PVC/OPF/PBCC samples. PVC showed the homogeneous and uniform surface. There were some voids in A1 and A2 samples, indicating the poor interaction of OPF along the PVC grid. Some of the OPF particles have been pulled away or became loose with PVC, resulting in bad stress transfer through the polymer and the filler. A superior distribution occurred at paltry PBCC content in PVC/OPF regarding A2 sample of 10 wt % PBCC and enhanced the interfacial adhesion of the components. When PBCC loadings increased in A3 and A4 samples, the distribution generates severe problems because of the agglomeration of PBCC particles related to its small size and high polar property. At greater percentages of PBCC in A5, the aggregated particles have a negative effect on the adhesion of PBCC along PVC, producing agglomeration sites and cavities inside the polymer matrix.[13,40]

3.5. Mechanical Outcomes. Tensile strength, tensile modulus, and strain at break of all composites are given in Table 6. Stress−strain curve confirmed the toughening behavior; strain at break, and tensile strength of PVC/OPF/PBCC compositions. The tensile strength of PVC is 41.76 MPa, giving ductile failure. On adding OPF, the failure mode immediately shifts from ductile to brittle, which is much stiffer. The tensile strengths of A1, A2, A3, A4, and A5 samples were 22.78, 29.21, 24.14, 21.06, and 20.85 MPa, respectively. This decrease compared to PVC may be due to the limitations imposed by OPF and PBCC molecular movements and poor interaction of OPF with PVC chains.[41,42] Fine and regular particles of PBCC improved the mechanical properties of PVC.[43] The tensile strengths of the A2 composite at 10 wt % PBCC and 50 wt % OPF are higher than that of A1, which has 60 wt % OPF; this may be due to the good distribution of PBCC particles in PVC and interfacial binding between polymer and filler, facilitating transfer of stress to the filler. Higher PBCC loadings lead to particle agglomeration and thus larger observed particles, which affect the toughness of the resultant composites and decrease the tensile strength of the A2, A3, and A4 samples. The tensile strength of A5 specimen indicating a better dispersion of PBCC than OPF particles in PVC. The olive pits flour induces swelling within the matrix, generating an important pressure deteriorating the mechanical properties. The tensile modulus of high OPF and/or PBCC loadings increased from 1164 MPa for PVC to 1455 for A1 and 2198 for A2, and then decreased to 1837 for A3, 1689 for A4, and 1617 MPa for A5. The increase of tensile modulus may be due to the restraining action of the fillers on PVC lattice. The A2 sample has the highest tensile modulus because PBCC particles strongly affect elastic modulus when incorporated in low contents, which results in a homogeneous dispersion of PBCC and less agglomeration in the PVC matrix. Tensile modulus decreased significantly from 2198 MPa for A2 to 1837, 1689, and 1617 MPa for A3, A4, and A5 composites, respectively. Dispersion becomes a severe problem that can be described as particles with higher dimension and smaller surface contact area that lead to development of cavities and interface debonding that affect the mechanical behavior of the polymer. The strain at break changed from 87.42% for PVC to 2.97% for A1, 3.11% for A2, 3.20% for A3, 3.36% for A4, and 3.65% for A5. This may be due to the effect of OPF and PBCC on the polymer chain mobility and the deformability of a rigid interface created between OPF/PBCC and PVC.[13,44]

Table 7 indicates that the principal values of notched strength of the Izod impact on composites PVC/OPF/PBCC are significantly reduced by the presence of OPF that diminishes PVC ductility and gives more frictional effects.[45] The impact strength of A2 is greater than those of A1, A3, A4, and A5 due to the finer PBCC dispersion in the PVC matrix. There were still some agglomerations at higher PBCC load levels, which led to larger observed particle size and gradually decreased impact strength.[46] With the inclusion of OPF in the matrix, the impact of PVC significantly decreases, progressively improves with the addition of 10 wt % PBCC, then decreases again significantly with the increase in PBCC content due to its agglomeration, and

https://doi.org/10.1021/acsomega.1c02932
ACS Omega 2021, 6, 23924−23933

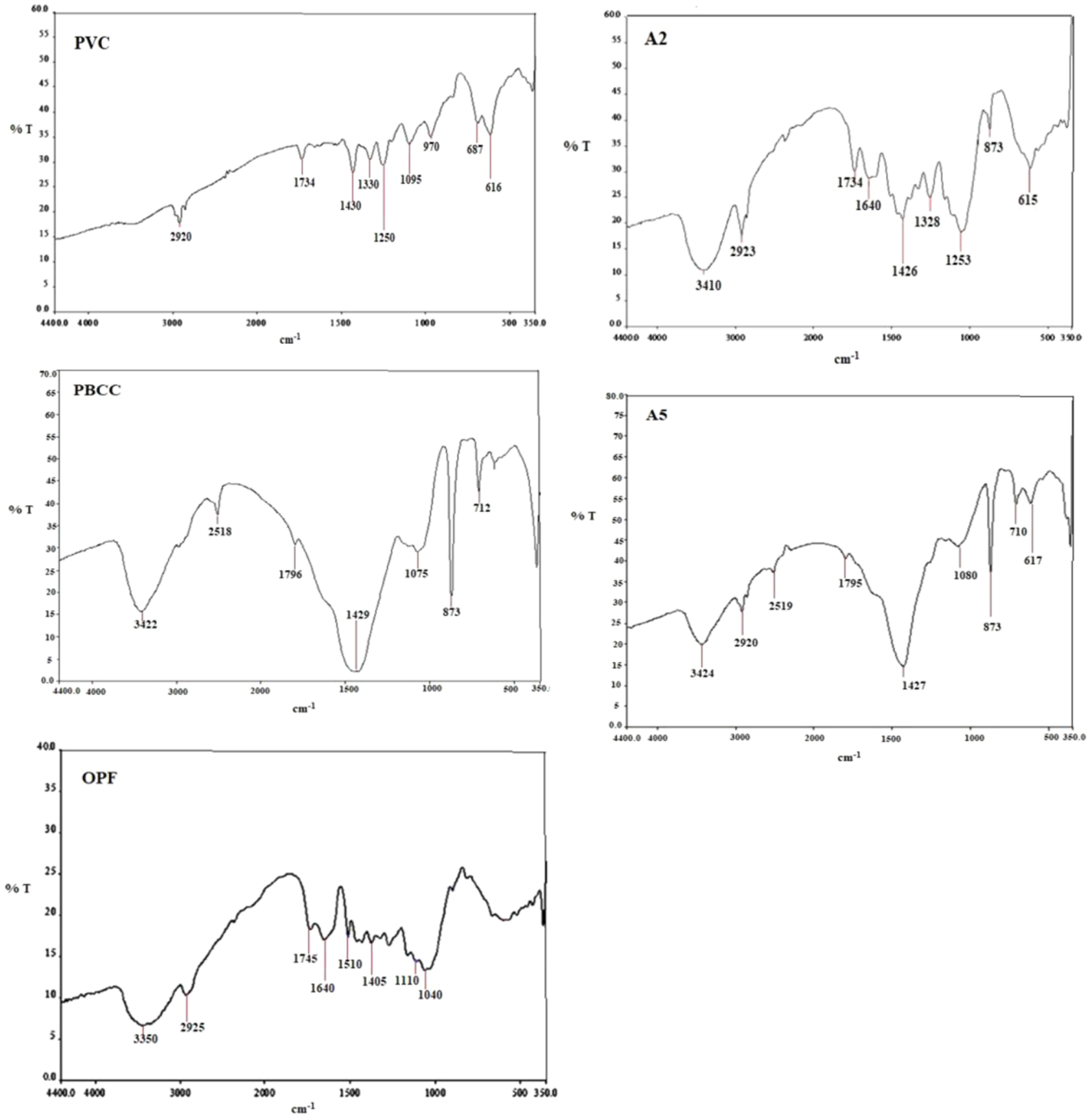

Figure 4. FTIR spectra of PVC, PBCC, OPF, A2, and A5.

affects the interfacial compatibility that allows the impact strength to be reduced.[13]

Table 8 indicates a decrease in flexural strength to 44.74 MPa for A1 due to a weak dispersion of fiber and a failure to adhere interfacially. Because of the fine distribution of PBCC particles into the matrix, the flexural strength of A2 is greater than those of A1, A3, A4, and A5. The A5 composite that includes 60 wt % PBCC gives a considerably higher value compared to A1 due to the absence of OPF.

Composites' hardness with OPF and PBCC applied greatly increases as shown in Table 9. Hardness increases considerably from 76 for A0 to 86 for A5 that may be clarified by the rigid characteristics of PBCC and OPF.

3.6. Water Absorption. H_2O absorption data of various components are obtained at various immersion times 2, 24, 168, 336, 672, and 1008 h. Hydrogen bonding sites are responsible for such results.[47] Table 10 represents that the absorption of H_2O of the A0 sample reached 0.38% after 1008 h of immersion, while the absorption for A1 was 15.68%, A2 was 12.28%, A3 was 9.24%, and A4 was 8.9%, and A5 was 0.75%. H_2O absorption in composites depends on the OPF loads. The H_2O absorption of composites is affected by high wt % of OPF. OPF comprises many free groups of hydroxyl (O−H) usable for contact water via hydrogen bonding. With increased OPF loading, water absorption in the composite systems increased drastically for three reasons: hydrogen bonding of H_2O molecules with $O\bar{H}$ in

https://doi.org/10.1021/acsomega.1c02932
ACS Omega 2021, 6, 23924−23933

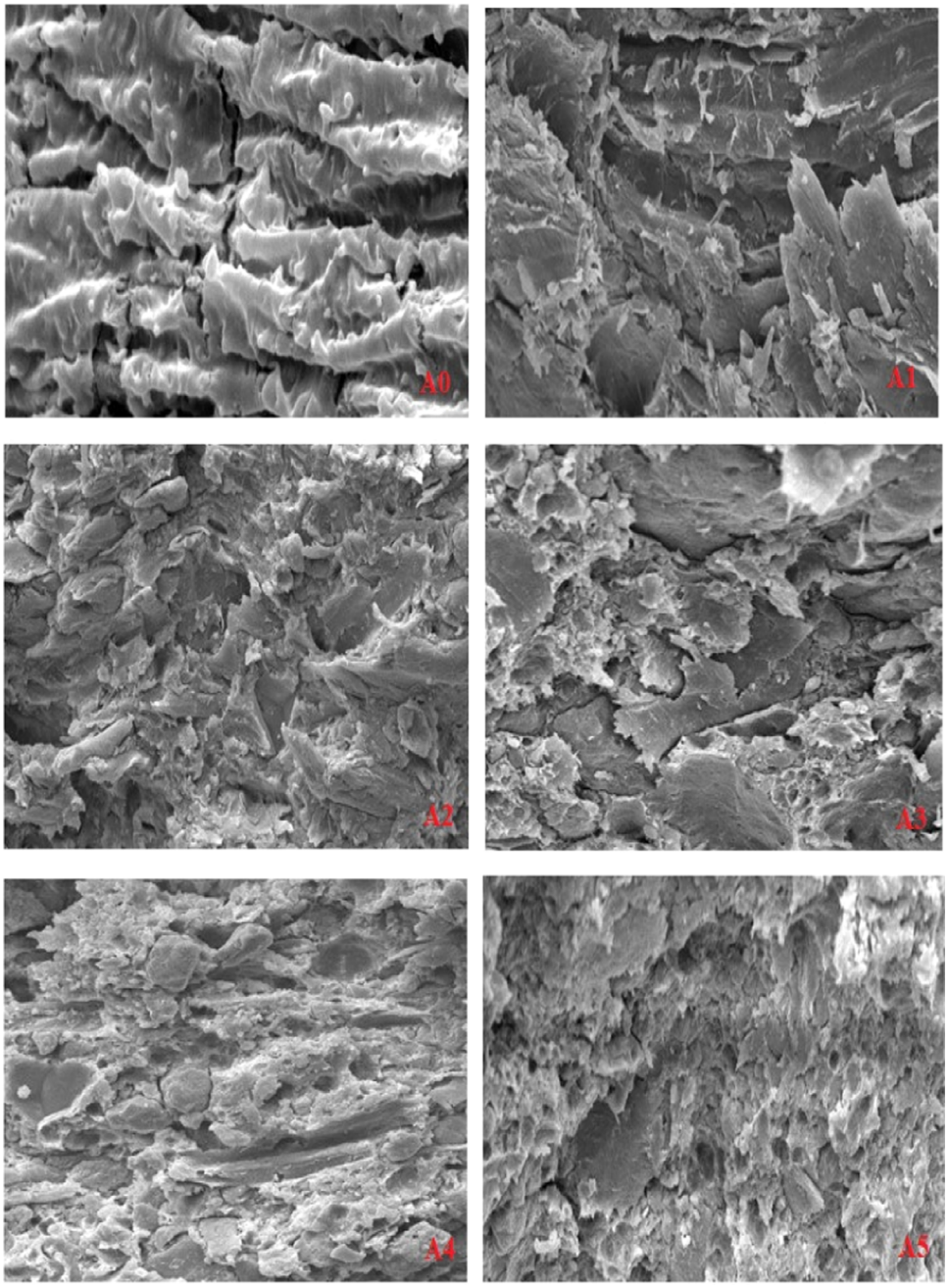

Figure 5. SEM images of fracture surfaces of PVC and its composites.

OPF, water molecule diffusion into the filler−matrix interfaces, and the broad variety of tubular pores in the fiber. The H_2O absorption of A1 composite was increased to 15.68% after 1008 h. In A2, voids and cavities decreased due to PBCC fine distribution, which improved the interface adhesion between filler and PVC matrix preventing the increase of absorbed H_2O.

Composite thickness swelling is similar to H_2O absorption. Composites showed high thickness swelling as shown in Figure 7. As cellulose is the principal component in OPF, absorbed H_2O is mainly located on a wooden fiber/polymer matrix interface. The thickness swelling of A0 increases from 0.31% after 2 h to 0.61% after 24 h and reached a constant value of 0.92% after 168 h until 1008 h because of the hydrophobic aspect of PVC. H_2O absorption increment is due to the compatibility of hydrophilic OPF and hydrophobic PVC. More water residential sites consumed more water with increasing wood content. The thickness swelling of A1 composites increased from 1.54% after 2 h to 3.41% after 24 h, 9.50% after 168 h, 14.52% after 336 h, 15.61% after 672 h, and 16.96% after 1008 h. The swelling of A2 composite was 1.37% after 2 h, 3.20% after 24 h, 7.84% after 167 h, 12.96% after 336 h, 13.98% after 672 h, and 14.19% after 1008 h. A5 has the lowest thickness swelling value of 0.57% after 2 h, 0.85% after 24 h, and then a constant value of 1.14% after 168 h until 1008 h due to lack of encapsulated filler of OPF and fine PBCC in a PVC matrix that shows no noticeable changes in the composite microstructure.

3.7. Specific Gravity (Sp.gr.). The influence of OPF and PBCC contents on the specific gravity of composites is explained in Table 11. The sp.gr. values of A0 and A1 composites were 1.44 and 1.40. The sp.gr. of A1 was not significantly affected because

https://doi.org/10.1021/acsomega.1c02932
ACS Omega 2021, 6, 23924−23933

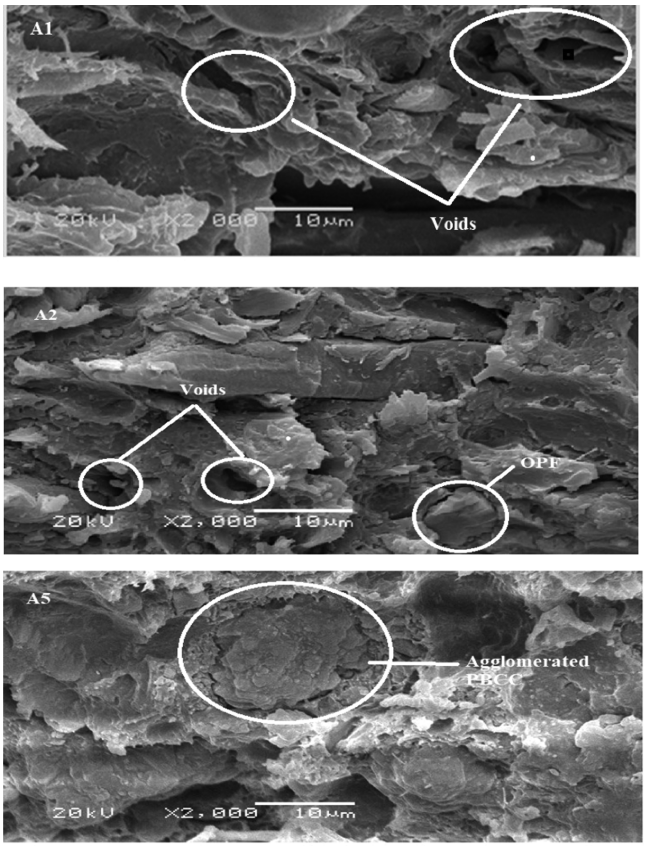

Figure 6. SEM images of fracture surfaces of A1, A2, and A5 composites.

Table 6. Tensile Strength, Tensile Modulus, and Strain at Break of PVC and Its Composites[a]

	property		
sample	tensile strength (MPa), $LSD_{0.05}$ = 1.39	tensile modulus (MPa), $LSD_{0.05}$ = 44.18	strain at break (%), $LSD_{0.05}$ = 0.81
A0	41.76^{A} (0.68)	1164^{F} (6.87)	87.42^{A} (0.08)
A1	22.78^{D} (0.84)	1455^{E} (9.77)	2.97^{B} (0.03)
A2	29.21^{B} (0.53)	2198^{A} (56.97)	3.11^{B} (0.01)
A3	24.14^{C} (0.25)	1837^{B} (6.87)	3.20^{B} (0.05)
A4	21.06^{E} (0.29)	1689^{C} (9.07)	3.36^{B} (0.49)
A5	20.85^{CD} (1.41)	1617^{D} (13.47)	3.65^{B} (0.15)

[a]Means with same letters in the same column are not significant, difference at 5% level of probability according to the least significant difference (LSD test).

Table 7. Izod Impact Resistance of PVC/OPF/PBCC Composites[a]

code samples	Notched Izod impact strength (J/m), $LSD_{0.05}$ = 1.08
A0	84.5^{A} (0.47)
A1	44.62^{E} (0.26)
A2	54.10^{B} (0.08)
A3	46.98^{D} (0.73)
A4	45.32^{E} (0.27)
A5	49.75^{C} (0.46)

[a]Means with same letters in the same column are not significant, difference at 5% level of probability according to the LSD test.

Table 8. Flexural Strength of PVC/OPF/PBCC Composites

code samples	flexural strength (MPa), $LSD_{0.05}$ = 0.38
A0	78.68^{A} (0.22)
A1	44.74^{E} (0.23)
A2	51.89^{B} (0.26)
A3	45.33^{D} (0.12)
A4	44.85^{E} (0.19)
A5	49.56^{C} (0.20)

Table 9. Shore-D Hardness of PVC/OPF/PBCC Composites[a]

code samples	hardness shore-D, $LCD_{0.05}$= 2.03
A0	76^{D} (0.55)
A1	79^{CD} (0.56)
A2	82^{AB} (0.8)
A3	83^{A} (1.97)
A4	85^{BC} (1.12)
A5	86^{CD} (1.12)

[a]Means with same letters in the same columns are not significant, difference at 5% level of probability according to the LSD test.

OPF has less bulk density than PVC. Sp.gr. increased by adding PBCC in more than 10% that may be due to the higher bulk density of PBCC than PVC. The sp.gr. values of A2, A3, A4, and A5 are 1.42, 1.58, 1.61, and 1.88, respectively. From A1 to A5, the weight of PBCC filler increased the matrix density.[40]

3.8. Thermal Characteristics. The TGA curves of A0, A1, A2, A3, A4, and A5 samples are listed in Table 12. The TGA curve for A0 has two weight loss stages in the range of 257−372 °C by 54.6% due to H−Cl elimination reaction and formation of polyene. Chlorine radicals are liberated from C−Cl bond scission taking off hydrogen radical from the adjacent C−H to produce the H−Cl bond. Such a mechanism generates double bonds in the polymer.[48] It develops via the chain according to the fact that every unsaturated bond dislocates the (Cl) atom in position with "allyl" activation resulting in H−Cl affecting the thermal stability without losing weight from 372 to 420 °C. Conjugated double bonds were obtained and a formed polyacetylene was more heat-stable than PVC because of cross-linking after forming. The second loss stage at 420−500 °C is much shorter than the first one corresponding to polyacetylene cracking. There are three stages of A1, A2, A3, and A4 composites decomposition. The first one is related to H_2O vaporization between 25.7 and 125 °C with weight losses of 5.9% for A1, 5.3% for A2, 4.5% for A3, and 3.3% for A4. This decrease in weight in this stage is related to the decrease in OPF content. Composites start to decompose after water vaporization at the second stage in the range of 238−372 °C for A1 with a weight loss of 55.8%, 240−372 °C for A2 with a weight loss of 51.6%, 243−372 °C for A3 with weight loss of 45.8%, and 244−372 °C for A4 with a weight loss of 38.9%. Composites begin to decompose at stage 3, which starts from 370 to 500 °C with weight loss of 17.9% for A1, 15.4% for A2, 16.2% for A3, and 12.5% for A4. The TGA curve of the A5 composite has three stages. The first stage starts in the range of 25.7−125 °C with a small weight loss of 1.5% due to the absorbed moisture. The second stage starts in the range of 246−357 °C with a weight loss of 21.9%, and the third stage starts in the range of 357−500 °C with a weight loss of 11.6%. In the range of 372−460 °C, the formed polyacetylene is more stable than PVC and hemicellulose decomposed, so the weight loss is observed for PVC/

https://doi.org/10.1021/acsomega.1c02932
ACS Omega 2021, 6, 23924−23933

Table 10. Water Absorption % of PVC/OPF/PBCC Composites[a]

	water absorption %					
sample	2 h	24 h	168 h	336 h	672 h	1008 h
A0	0.13^{D} (0.007)	0.15^{E} (0.001)	0.22^{E} (0.002)	0.37^{E} (0.087)	0.38^{E} (0.087)	0.38^{E} (0.085)
A1	1.76^{A} (0.018)	4.22^{A} (0.242)	10.79^{A} (0.001)	14.33^{A} (0.164)	15.07^{A} (0.052)	15.68^{A} (0.105)
A2	1.18^{B} (0.017)	3.15^{A} (0.112)	8.24^{B} (0.135)	11.21^{B} (0.011)	11.64^{B} (0.318)	12.28^{B} (0.521)
A3	1.08^{B} (0.087)	2.91^{B} (0.102)	8.03^{B} (1.003)	8.85^{C} (0.088)	8.94^{C} (0.499)	9.24^{C} (0.082)
A4	0.94^{C} (0.037)	2.52^{C} (0.249)	6.86^{C} (1.005)	8.52^{C} (0.231)	8.73^{C} (0.025)	8.86^{C} (0.138)
A5	0.31^{D} (0.009)	0.37^{D} (0.007)	0.46^{D} (0.035)	0.74^{D} (0.058)	0.75^{D} (0.058)	0.75^{D} (0.057)

[a]Means with same letters in the same column are not significant, difference at 5% level of probability according to the LSD test.

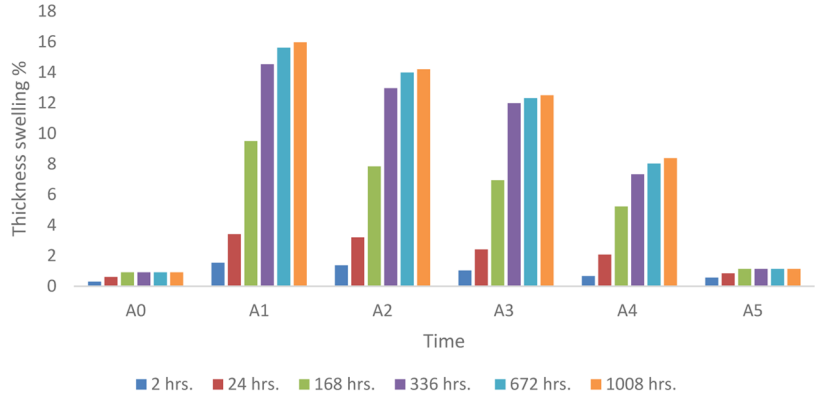

Figure 7. Thickness swelling (%) of PVC and PVC/OPF/PBCC composites.

Table 11. Specific Gravities of the Prepared Composites[a]

code samples	Sp.gr., $LSD_{0.05}$ = 0.18
A0	1.44^{C} (0.01)
A1	1.40^{D} (0.02)
A2	1.42^{D} (0.02)
A3	1.58^{B} (0.01)
A4	1.61^{B} (0.02)
A5	1.88^{A} (0.01)

[a]Means with same letters in the same column are not significant, difference at 5% level of probability according to the LSD test.

OPF composites, leaving a stable PVC in this temperature range.[49,50] In this range of temperature, organic impurities in PBCC may decompose while the PVC compound remains stable. The onset of decomposition temperature of the PVC compound decreased with the addition of either OPF or PBCC. This is because of the filler content inducing defects in the form of aggregates and heterogeneities in the polymer matrix. The decomposition onset temperatures for A2, A3, A4, and A5 composites were lower than that of neat PVC. The thermal stability of such composites is enhanced because of the small particles size of PBCC compared with OPF particle size and the total surface contact area of PBCC particles/PVC matrix is more than that of OPF particles/PVC matrix. The PVC matrix can be protected from heat, and PBCC may act as an acid acceptor adding stabilization for PVC and neutralization of Cl^{-}. PBCC has a high surface area because of small particle size.

The most important temperature-dependent property for amorphous polymers is the glass-transition temperature (T_g), the temperature at which the polymer changes from a relatively brittle material to a softer plastic material, which was determined by differential scanning calorimetry (DSC). The DSC curves in Figure 8 showed T_g's of A0, A1, A2, A3, A4, and A5 at 85, 92.3, 93.7, 92.8, 91.9, and 92.8 °C, respectively. The increase of T_g after adding OPF may be due to the polar−polar interactions between PVC and olive pits flour molecules forming strong hydrogen bonds, which prohibit the chain mobility. In addition, the homogeneous distribution of PBCC in the PVC matrix is the driving force that increases the T_g of the PVC/PBCC composites prohibiting the molecular chain movement of PVC.[13]

Table 12. Decomposition Stages and Weight Loss of PVC/OPF/PBCC

decomposition stage	first			second			third			
composites	start (°C)	end (°C)	wt loss (%)	start (°C)	end (°C)	wt loss (%)	start (°C)	end (°C)	wt loss (%)	total residue (%) at temp. 500 °C
A0				257	372	54.6	420	500	12.46	32
A1	25.7	125	5.9	238	372	55.8	372	5500	17.9	20.4
A2	25.7	125	5.3	240	372	51.6	372	5500	15.4	27.7
A3	25.7	125	4.5	243	372	45.8	372	500	16.2	33.5
A4	25.7	125	3.3	244	372	38.9	372	500	12.5	45.3
A5	25.7	125	1.5	246	357	21.9	357	500	11.6	65

https://doi.org/10.1021/acsomega.1c02932
ACS Omega 2021, 6, 23924−23933

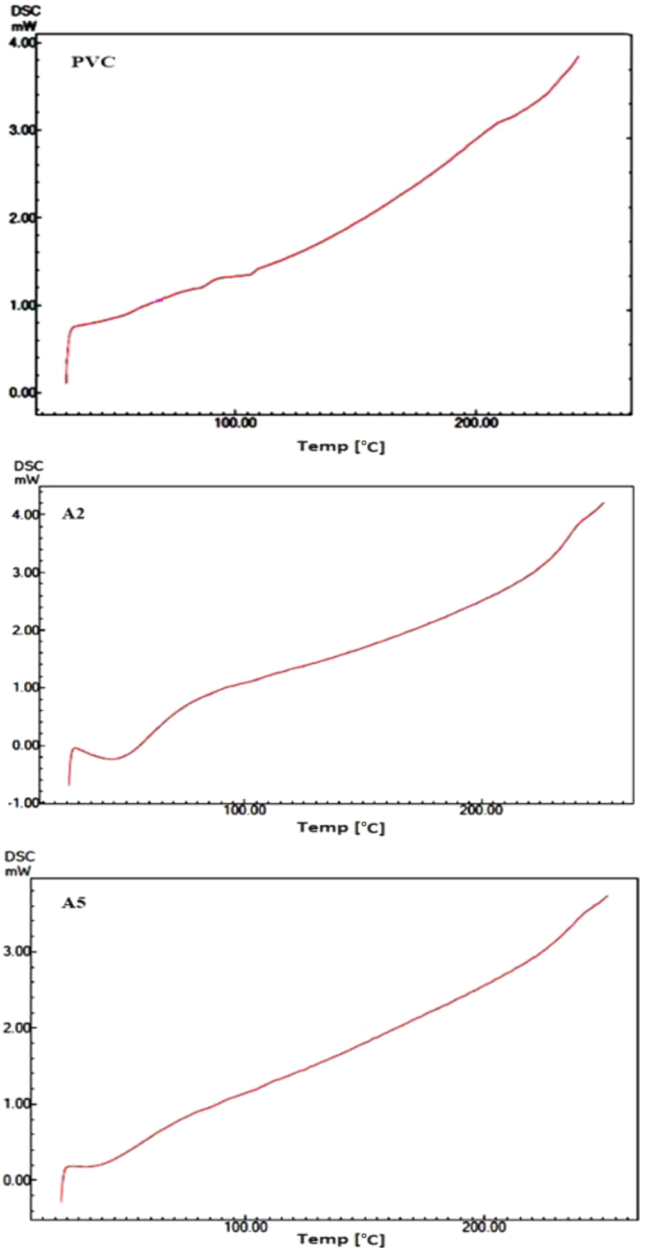

Figure 8. DSC curves of PVC, A2, and A5.

4. CONCLUSIONS

For keeping the environment clean, low-cost wastes olive pits flour and precipitated bio-calcium carbonate were successfully used as fillers in PVC. The formed composites have superior thermal stability, stiffness, and physical and mechanical properties compared to PVC. It was found that the tensile modulus, hardness, and flexural strength increased by the incorporation of both PBCC and OPF into the PVC matrix. The uniform distribution of PBCC in the PVC/OPF composite is a major factor responsible for the improvement of the mechanical properties. Water uptake and thickness swelling of PVC/OPF/PBCC composites were higher than those of the PVC compound due to the polarity of OPF. The thermal stability of composites containing PBCC is enhanced because of the smaller particle size of PBCC compared to OPF particle size. The contact surface area between OPF particles and PVC matrix is much smaller than that between PBCC particles and PVC matrix. PBCC may act as an acid acceptor for extra stabilization of PVC and neutralization of Cl^- ions. The characteristics of the A2 composite were improved by adding a low content of PBCC that may be due to the fine dispersion PBCC in the PVC matrix. The uniform distribution of PBCC in the PVC/OPF composite is a major factor responsible for the enhancement of most properties. In the future work, different ways may be investigated to improve the PBCC dispersion at higher contents than 10 wt % aiming to decrease the cost of processing such composites.

AUTHOR INFORMATION

Corresponding Author

Salah F. Abdellah Ali − *Department of Chemistry, College of Science and Arts, Jouf University, Gurayat 77217, Saudi Arabia; Materials Science Department, Institute of Graduate Studies & Research, Alexandria University, Alexandria 21526, Egypt;* orcid.org/0000-0002-6672-4111; Email: sfali@ju.edu.sa

Authors

Ibrahim O. Althobaiti − *Department of Chemistry, College of Science and Arts, Jouf University, Gurayat 77217, Saudi Arabia*

E. El-Rafey − *Materials Science Department, Institute of Graduate Studies & Research, Alexandria University, Alexandria 21526, Egypt*

Ehab S. Gad − *Department of Chemistry, College of Science and Arts, Jouf University, Gurayat 77217, Saudi Arabia; Chemistry Department, Faculty of Science, Al-Azhar University, Cairo 11884, Egypt*

Complete contact information is available at: https://pubs.acs.org/10.1021/acsomega.1c02932

Notes

The authors declare no competing financial interest.

ACKNOWLEDGMENTS

The authors extend their appreciation to the Deanship of Scientific Research at Jouf University for funding this work through research grant no. DSR2020-01-521.

REFERENCES

(1) Ali, S. F. A. Biodegradation properties of poly-ε-caprolactone, starch and cellulose acetate butyrate composites. *J Polym. Environ.* **2014**, *22*, 359−64.

(2) Abdellah-Ali, S. F. Mechanical and thermal properties of promising polymer composites for food packaging applications. In *IOP Conference Series: Materials Science and Engineering*; IOP Publishing, 2016; Vol. *137*, p 012035.

(3) Abdellah-Ali, S. F.; Hassan, W. K. Investigation and Evaluation of Poly (n-butyl acrylate) for Oil Fractions Spill Removal Applications. *Egypt. J. Chem.* **2020**, *63*, 15−25.

(4) Abdellah-Ali, S. F. Performance of cellulose acetate propionate in polycaprolactone and starch composites: biodegradation and water resistance properties. *Biointerface Res. Appl. Chem.* **2020**, *10*, 5382−6.

(5) Migneault, S.; Koubaa, A.; Erchiqui, F.; Chaala, A.; Englund, K.; Wolcott, M. P. Effects of processing method and fiber size on the structure and properties of wood−plastic composites. *Composites, Part A* **2009**, *40*, 80−5.

(6) El-Rafey, E.; Walid, W. M.; Syala, E.; Ezzat, A. A.; Abdellah-Ali, S. F. A study on the physical, mechanical, thermal properties and soil biodegradation of HDPE blended with PBS/HDPE-g-MA. *Polym. Bull.* **2021**, *175*, No. 109126.

(7) Abd El-Rahman, K. M.; Abdellah Ali, S. F.; Khalil, A. I.; Kandil, S. Influence of poly(butylene succinate) and calcium carbonate nano-

particles on the biodegradability of high density-polyethylene nanocomposites. *J Polym Res.* **2020**, *27*, No. 231.
(8) Abdellah-Ali, S. F. Performance of cellulose acetate propionate in polycaprolactone and starch composites: biodegradation and water resistance properties. *Biointerface Res. Appl. Chem.* **2020**, *10*, 5382−6.
(9) Ali, S. F. A.; Elsad, R. A.; Mansour, S. A. Enhancing the dielectric properties of compatibilized high-density polyethylene/calcium carbonate nanocomposites using high-density polyethylene-g-maleic anhydride. *Polym. Bull.* **2021**, *78*, 1393−405.
(10) Fink, J. K. *Aconcise Introduction to Additives for Thermoplastic Polymers*, 1st ed.; John Wiley & Sons, 2010; Vol. *1*.
(11) Stuart, P. *PVC Compounds and Processing*; Rapra Technology Limited: United Kingdom, 2004; Vol. *15*.
(12) Xu, Y.; Wu, Q.; Lei, Y.; Yao, F.; Zhang, Q. Natural fiber reinforced poly (vinyl chloride) composites: Effect of fiber type and impact modifier. *J. Polym. Environ.* **2008**, *16*, 250−7.
(13) Abdellah-Ali, S. F.; Mervette, E. B.; Abdelhamed, M.; El-Rafey, E. Formulation and characterization of new ternary stable composites: Polyvinyl chloride-wood flour-calcium carbonate of promising physicochemical properties. *J. Mater. Res. Technol.* **2020**, *9*, 12840−12854.
(14) Titow, M. V. *PVC Technology*; Springer Science & Business Media, 2012.
(15) Mishra, S. B.; Mishra, A. K.; Kaushik, N. K.; Khan, M. A. Study of performance properties of lignin-based polyble nnds with polyvinyl chloride. *J. Mater. Process. Technol.* **2007**, *183*, 273−276.
(16) Gilbert, M.; Patrick, S. *Poly(vinyl chloride)*; Brydson's Plastics Materials, 2017; pp 1−18.
(17) Liefke, E. Recent Developments of PVC Compounds for Special Applications. In PVC-Formulation Conference (AMI), Cologne, Germany, 2009.
(18) Jariwala, H.; Jain, P. A review on mechanical behavior of natural fiber reinforced polymer composites and its applications. *J. Reinf. Plast. Compos.* **2019**, *38*, 441−53.
(19) Joshi, P. S.; Marathe, D. S. Mechanical properties of highly filled PVC/wood-flour composites. *J. Reinf. Plast. Compos.* **2010**, *29*, 2522−33.
(20) Yáñez-Pacios, A. J.; Martín-Martínez, J. M. Surface modification and adhesion of wood-plastic composite (WPC) treated with UV/ozone. *Compos. Interfaces* **2018**, *25*, 127−149.
(21) Zhou, Y.; Fan, M.; Chen, L. Interface and bonding mechanisms of plant fibre composites: An overview. *Composites, Part B* **2016**, *101*, 31−45.
(22) Altun, Y.; Doğan, M.; Bayramli, E. Comparative study of maleated and glycidyl methacrylate functionalized terpolymers as compatibilizers for low-density polyethylene−wood flour composites. *J. Appl. Polym. Sci.* **2013**, *127*, 1010−1016.
(23) Matuana, L. M. Recent developments in wood plastic composites. *J. Vinyl Addit. Technol.* **2009**, *15*, 136−138.
(24) Sombatsompop, N.; Prapruit, W.; Chaochanchaikul, K.; Pulngern, T.; Rosarpitak, V. Effects of cross section design and testing conditions on the flexural properties of wood/PVC composite beams. *J. Vinyl Addit. Technol.* **2010**, *16*, 33−41.
(25) Bahari, S. A.; Warren, J. G.; Andreas, K. Thermal stability of processed PVC/bamboo blends: effect of compounding procedures. *Eur. J. Wood Prod.* **2017**, *75*, 147−159.
(26) Gozdecki, C. E.; Wilczynski, A. *Effect of Wood Flour Type on Tensile Properties of Wood-Polymer Composites*; Annals of Warsaw University of Life Sciences-SGGW. Forestry and Wood Technology, 2015; Vol. *91*.
(27) Najafi, S. K. Use of recycled plastics in wood plastic composites−A review. *Waste Manag.* **2013**, *33*, 1898−905.
(28) Dairi, B.; Djidjelli, H.; Boukerrou, A. Study and characterization of composites materials based on polyvinyl chloride loaded with wood flour. *J. Mater. Sci. Eng. A* **2013**, *3*, 110−116.
(29) Farsheh, A. T.; Talaeipour, M.; Hemmasi, A. H.; Khademieslam, H.; Ghasemi, I. Investigation on the mechanical and morphological properties of foamed nanocomposites based on wood flour/PVC/multi-walled carbon nanotube. *Bioresources* **2011**, *6*, 841−52.
(30) Azwa, Z. N.; Yousif, B. F.; Manalo, A. C.; Karunasena, W. A review on the degradability of polymeric composites based on natural fibres. *Mater. Des.* **2013**, *47*, 424−42.
(31) Ashori, A. Wood−plastic composites as promising green-composites for automotive industries. *Bioresour. Technol.* **2008**, *99*, 4661−7.
(32) John, M. J.; Thomas, S. Biofibres and biocomposites. *Carbohydr. polym.* **2008**, *71*, 343−64.
(33) Cornwell, D. W. Benefits of PCC as a PVC Additive. In Third Minerals in Compounding Conference, Cologne, Germany, pp 35−37, 2001.
(34) Guffey, V. O.; Sabbagh, A. B. PVC/wood-flour composites compatibilized with chlorinated polyethylene. *J. Vinyl Addit. Technol.* **2002**, *8*, 259−263.
(35) Chen, Y.; Chiparus, O.; Sun, L.; Negulescu, I.; Parikh, D. V.; Calamari, T. A. Natural fibers for automotive nonwoven composites. *J. Ind. Text.* **2005**, *35*, 47−62.
(36) Rowell, D. L. *Soil Science: Methods & Applications*; Routledge, 2014.
(37) Saini, G.; Choudhary, V.; Bhardwaj, R.; Narula, A. K. Study on PVC composites containing Eugenia jambolana wood flour. *J. Appl. Polym. Sci.* **2008**, *107*, 2171−2179.
(38) Yanming, C.; Jungang, L.; Meng, Z.; Wen, Z.; Yong, L.; Zhaohong, W.; Jimin, F. Discrimination of Carbonate-Containing and Carbonate-Free Polyvinyl Chloride with Fourier Transform Infrared Microscopy and Raman Spectroscopy. *Spectroscopy* **2012**, *27*, 36−41.
(39) Yang, Z.; Yang, H.; Yang, H. Effects of sucrose addition on the rheology and microstructure of κ-carrageenan gel. *Food Hydrocolloids* **2018**, *75*, 164−73.
(40) Bai, X. Y.; Wang, Q. W.; Sui, S. J.; Zhang, C. S. The effects of wood-flour on combustion and thermal degradation behaviors of PVC in wood-flour/poly (vinyl chloride) composites. *J. Anal. Appl. Pyrolysis* **2011**, *91*, 34−9.
(41) Liu, P.; Zhao, M.; Guo, J. Thermal stabilities of poly (vinyl chloride)/calcium carbonate (PVC/CaCO3) composites. *J. Macromol. Sci., Part B: Phys.* **2006**, *45*, 1135−40.
(42) Bouhamed, N.; Souissi, S.; Marechal, P.; Amar, M. B.; Lenoir, O.; Leger, R.; Bergeret, A. Ultrasound evaluation of the mechanical properties as an investigation tool for the wood-polymer composites including olive wood flour. *Mech. Mater.* **2020**, *148*, No. 103445.
(43) Kemal, I.; Whittle, A.; Burford, R.; Vodenitcharova, T.; Hoffman, M. Toughening of unmodified polyvinylchloride through the addition of nanoparticulate calcium carbonate. *Polymer* **2009**, *50*, 4066−79.
(44) Ramli, R. A.; Zakaria, N. Z.; Rahman, U. U.; Bakhtiar, N. B.; Mustapha, S. N.; Lian, Y. M. Effect of mineral fillers on mechanical, thermal and morphological properties of kenaf recycled polyethylene wood plastic composite. *Eur. J. Wood Prod.* **2018**, *76*, 1737−43.
(45) Shojaeiarani, J.; Bajwa, D. S.; Stark, N. M. Green esterification: A new approach to improve thermal and mechanical properties of poly (lactic acid) composites reinforced by cellulose nanocrystals. *J. Appl. Polym. Sci.* **2018**, *135*, 46468.
(46) Michael, A. *Materials Selection in Mechanical Design Book*, 4th ed.; Elsevier-India, 2011.
(47) Ashori, A.; Nourbaksh, A. Performance properties of micro-crystalline cellulose as a reinforcing agent in wood plastic composites. *Composites, Part B* **2010**, *41*, 578−581.
(48) Akay, M. *Introduction to Polymer Science and Technology Book*; Ventus Publishing Aps: N. Ireland, 2012.
(49) Poletto, M.; Zattera, A. J.; Forte, M. M.; Santana, R. M. Thermal decomposition of wood: Influence of wood components and cellulose crystallite size. *Bioresour. Technol.* **2012**, *109*, 148−153.
(50) Fang, Y.; Wang, Q.; Bai, X.; Wang, W.; Cooper, P. A. Thermal and burning properties of wood flour-poly (vinyl chloride) composite. *J. Therm. Anal. Calorim.* **2012**, *109*, 1577−85.

https://doi.org/10.1021/acsomega.1c02932
ACS Omega 2021, 6, 23924−23933